

## Evidence for Transient Electric Field Gradients in H-like Ions Traversing Gd Targets at High Velocities

U. Grabow,<sup>1</sup> K.-H. Speidel,<sup>1</sup> J. Cub,<sup>2</sup> H. Busch,<sup>1</sup> H.-J. Wollersheim,<sup>2</sup> G. Jakob,<sup>3</sup> A. Gohla,<sup>1</sup>  
J. Gerber,<sup>4</sup> and M. Loewe<sup>5</sup>

<sup>1</sup>*Institut für Strahlen- und Kernphysik, Universität Bonn, Nussallee 14-16, D-53115 Bonn, Germany*

<sup>2</sup>*Gesellschaft für Schwerionenforschung, Postfach 110552, D-64220 Darmstadt, Germany*

<sup>3</sup>*Physik-Dept. Technische Universität München, James-Frank-Str., D-85748 Garching, Germany*

<sup>4</sup>*Institut de Recherches Subatomique, F-67037 Strasbourg, France*

<sup>5</sup>*Sektion Physik Ludwig-Maximilians-Universität München, D-85748 Garching, Germany*

(Received 23 May 1997)

Transient electric field gradients have been observed in measurements of particle- $\gamma$ -angular correlations of Coulomb excited nuclei in H-like ions during traversal through thick metallic layers. The  $V_{ZZ}$  values deduced for  $^{20}\text{Ne}(2^+)$ ,  $^{32}\text{S}(2^+)$ ,  $^{40}\text{Ar}(2^+)$ ,  $^{52}\text{Cr}(2^+)$ ,  $^{54}\text{Fe}(2^+)$ , and  $^{62}\text{Ni}(2^+)$  are found to be of the order of  $10^{21}$  V/cm<sup>2</sup> with consistently positive sign. They arise from distortions of the  $1s$  electron orbit of the H-like ions by the wake field gradient induced in the solid by the charge of the moving ion. The observed interaction frequencies reflect the sign of the quadrupole moment of the excited  $2^+$  states. [S0031-9007(97)04775-3]

PACS numbers: 21.10.Ky, 23.20.En, 24.70.+s, 61.80.-x

Considerable interest in strong electric field gradients has been expressed in particular with respect to nuclei at high angular momenta to determine sign and magnitude of quadrupole moments of states with ps lifetimes. A measurement of such quadrupole moments can be achieved only with field gradients having strengths of  $10^{21}$  V/cm<sup>2</sup>; the field gradients accessible at impurities implanted in noncubic crystalline lattices are (3–4) orders in magnitude smaller and therefore unsuitable for the nuclear lifetimes in question.

Very strong electric field gradients of transient nature (TEFG) have been predicted a long time ago for fast moving ions in solids [1]. Their origin is associated with the slowing down force generated by a strong induced electric field or so-called wake field [2] which must also have a gradient [3]. This gradient will act on the electron shells of the moving ion leading to Sternheimer-like enhancements at the nucleus. Its interaction with the nuclear quadrupole moment during the transit or stopping time in the solid will cause perturbations in the angular correlation of decay  $\gamma$  rays emitted by the nucleus. This perturbed angular correlation (PAC) technique has been used so far in three different experiments [3–5] which yielded only upper limits of the corresponding TEFGs in agreement with theoretical estimates. The latter are based on the assumption that the axially symmetric wake field gradient with the  $z$  axis in the direction of the moving ion  $V_{ZZ}^{\text{wake}}$  will cause distortions of the electron shells giving rise to very intense TEFG at the nucleus.  $V_{ZZ}^{\text{wake}}$  results from electron density oscillations induced in the solid by the charge of the moving ion, as illustrated in Fig. 1 (see also [2]). It can be expressed by

$$V_{ZZ}^{\text{wake}}(R=0, z=v_{\text{ion}}t) = -\frac{m_e e}{\hbar} \frac{Z_{\text{eff}}}{v_{\text{ion}}} \omega_p^2, \quad (1)$$

where  $Z_{\text{eff}}$  is the effective charge of the ion at the velocity  $v_{\text{ion}}$ ,  $z$  the longitudinal distance in the rest frame of the moving ion, and  $\omega_p$  the plasma frequency of the solid. The latter is given by

$$\omega_p = \frac{2\pi v_{\text{ion}}}{\lambda_w}, \quad (2)$$

where  $\lambda_w$  is the wavelength of the wake. The magnitude of  $V_{ZZ}^{\text{wake}}$  is typically of the order of  $10^{17}$  V/cm<sup>2</sup>.

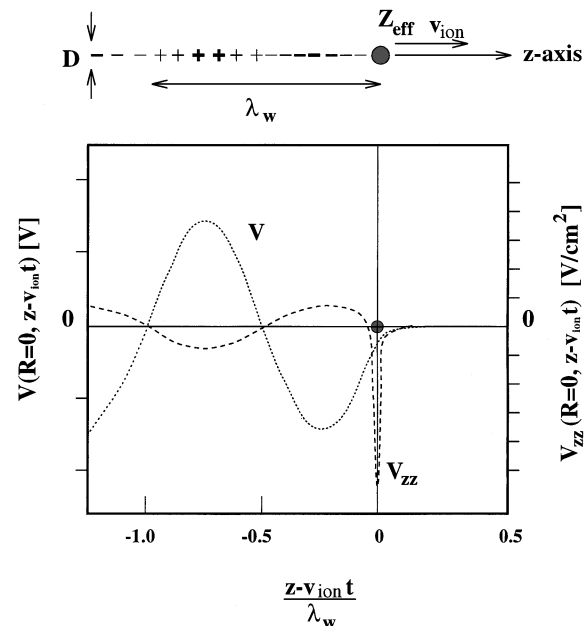


FIG. 1. Schematic distribution of the wake potential and its second derivative along the track ( $z$ -axis) of the ion with effective charge  $Z_{\text{eff}}$ . The wavelength  $\lambda_w$  and the transversal extension  $D$  of the wake are indicated [2,4].

At velocities  $v_{\text{ion}} \approx Zv_0$  ( $v_0 = c/137$ ) where the ions are predominantly in the H-like charge state, the distortion by the wake field gradient concerns the  $1s$  electron orbit. Because of the  $1/r^3$  dependence of  $V_{ZZ}$ , an assumed displacement of the  $1s$  electron orbit from the nucleus by approximately one orbital radius will lead to a very large field gradient of the  $K$  shell which has been considered as an upper limit [3]:

$$V_{ZZ}^K = \frac{16eZ^3}{27a_0^3} = 5.8Z^3 \times 10^{17} \text{ V/cm}^2, \quad (3)$$

where  $a_0$  is the Bohr radius. This field gradient has a positive sign directly reflecting the Sternheimer effect which inverts the sign of the wake field gradient as for crystalline field gradients [see Eq. (1) and [6]].

A main source of difficulties in two of the above-mentioned measurements was due to the presence of strong magnetic hyperfine interactions (HFI) acting on the ions when they emerge from the target into vacuum. These HFI cause attenuations of the angular correlation which reduce the sensitivity to the TEFG. With respect to suitable experimental conditions H-like ions are definitely preferred. Moreover, the disturbing influence by the magnetic HFI should be minimized, which requires that the passage time of the ions through the solid is larger or comparable to the nuclear lifetime of the excited state and/or its magnetic moment is small. Another requirement for sensitive detection of electric quadrupole interactions (EQI) is sufficient polarization of the nuclear state. This condition is well fulfilled in Coulomb scattering of the ions at angles  $\Theta_P < \pi$  (see Fig. 2) as discussed in [3,7], which enables us to measure also the sign of quadrupole moments in contrast to standard PAC technique.

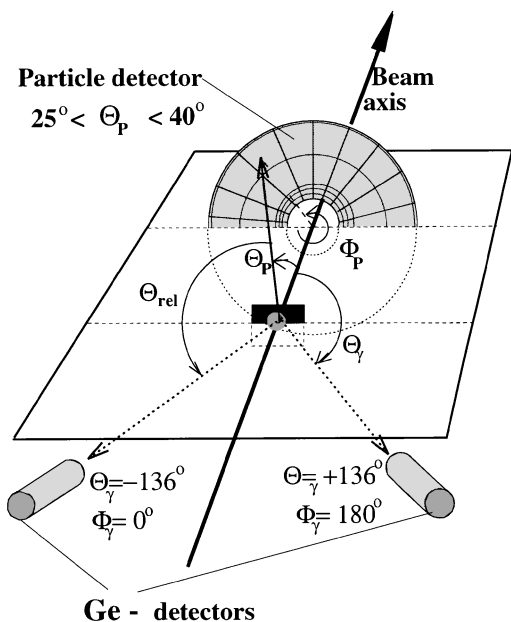


FIG. 2. Schematic view of the detector arrangement in the  $\gamma$ -detection plane. Only one pair of Ge detectors placed symmetric to the beam direction is shown.

We report here on particle- $\gamma$ -angular correlation data of various nuclei obtained in measurements following Coulomb excitation (C.E.) of the first  $2^+$  state at velocities where the ions are in the favorable  $1s$  electron configuration. All these measurements have in common the fact that they were planned to determine, in particular, the transient magnetic fields (TF) for ions at high velocities [8]. This also explains why ferromagnetic Gd and Fe were used as target material with the knowledge of the  $\gamma$ -angular correlation being crucial for determining the nuclear spin precession in the TF. It is noted that the TF part of these measurements has already been reported:  $^{20}\text{Ne}(2^+)$  [9],  $^{32}\text{S}(2^+)$  [5],  $^{40}\text{Ar}(2^+)$  [10],  $^{52}\text{Cr}(2^+)$  [11],  $^{54}\text{Fe}(2^+)$  [12], and  $^{62}\text{Ni}(2^+)$  [13]. Detailed particle- $\gamma$ -angular correlations have been measured for all these nuclei but contributions from EQI of TEFG were not explicitly included in the analysis with the exception of [5] and [11]. This omission has now been retrieved. It should be emphasized that the effect of the TF precession on the  $\gamma$ -angular correlations has been eliminated by averaging the individual correlations measured for *up* and *down* directions of the external magnetic field. Hence, for the further discussion of EQI only these (TF *free*) angular correlations were used.

In view of favorable conditions for TEFG, the measurements on  $^{32}\text{S}(2^+)$  [5] turn out to be a test case, as its quadrupole moment  $Q(2^+) = -0.149(13) e b$  and in particular its short lifetime  $\tau = 0.246(9)$  ps render it very suitable. Furthermore, the measured angular correlations are of high precision, which made a reanalysis particular profitable. The procedure described below has been applied in a consistent way to the data of all other nuclei as well. It is also noted that the former analysis of the same  $^{32}\text{S}(2^+)$  data yielded only an upper limit of a TEFG, which is related to erroneous solid angle corrections for the Ge detectors used leading to an underestimation of the TEFG.

In the measurements with  $^{32}\text{S}$  ions [5] particle- $\gamma$ -angular correlations were obtained from counting rate ratios of two independent pairs of Ge detectors placed at fixed angles ( $\Theta_\gamma = \pm 31^\circ, \pm 136^\circ$ ) symmetric to the beam direction (Fig. 2). These ratios were measured as a function of the azimuth angle  $\Phi_P$  defined by 20 sections of the ion detector. The latter was an annular parallel plate avalanche gas counter with an acceptance angle of  $25^\circ \leq \Theta_P^{\text{lab}} \leq 40^\circ$  for the forward scattered  $^{32}\text{S}$  ions. As a result, the Coulomb excited  $2^+$  state at 2.229 MeV became sufficiently polarized. The target consisted of a  $10.5 \text{ mg/cm}^2$  thick Gd layer deposited on a  $1.0 \text{ mg/cm}^2$  Ta foil sandwiched between thin Cu layers ( $1 \text{ mg/cm}^2$ ) for thermal reasons. The excitation of the 262 MeV  $^{32}\text{S}$  ions essentially took place in Ta/Gd implying an effective time in the target of  $T = 0.31(3)$  ps at the mean velocity  $v_{\text{ion}} \approx 16v_0$ . The latter has been calculated considering the formation and decay of the nuclear probe in the Ta/Gd layers using stopping powers [14] in the kinematical conditions and the known nuclear lifetime. During this time EQI with the TEFG are experienced causing specific changes in the angular correlation which depend on the sign of the field gradient as

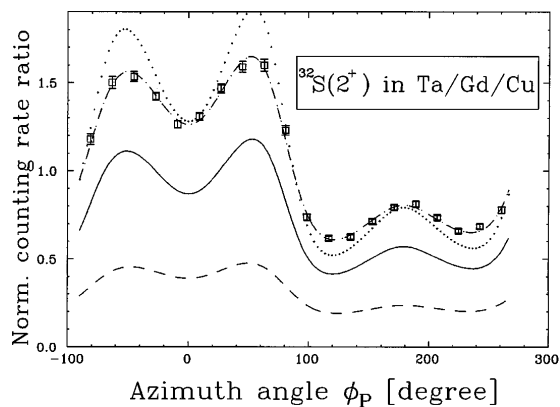


FIG. 3. Measured particle- $\gamma$ -angular correlation ( $\Theta_\gamma = \pm 136^\circ$ ) for  $^{32}\text{S}(2^+)$  ions with least squares fit to the data [Eq. (4)]. The other curves refer to the unperturbed correlation (dotted line) and the two separated contributions due to EQI only (solid line) and additional magnetic HFI (dashed line).

well. It should be emphasized that in these conditions  $\approx 70\%$  of the ions are exposed only to a possible TEFG of the Ta-Gd-Cu layers of the target while the remaining ions experience both EQI and magnetic HFI on emergence into vacuum. Such a high sensitivity to TEFG does not exist in the other cases studied.

Figure 3 shows angular correlation data of one detector pair in the rest frame of the  $\gamma$ -emitting nuclei together with results from COULEX calculations using the Winther-de Boer code [15]. Also displayed are the relative contributions to the measured correlation from ions *inside* (only EQI) and *outside* the target (EQI plus magnetic HFI) reflecting the specifically large sensitivity to TEFG.

For describing the data the generalized expression of the angular correlation function has been used which is given by [15,16]

$$W(\Theta_\gamma, \Phi_\gamma, \Phi_P, t) = \sum_{kq} \rho_{kq}(t) F_k Q_k Y_{kq}(\Theta_\gamma, \Phi_\gamma, \Phi_P), \quad (4)$$

where  $F_k$  are the angular correlation coefficients of the ( $2^+ \rightarrow 0^+$ )  $\gamma$  transition, the  $Q_k$  account for the solid angle of the  $\gamma$  detectors used and the  $Y_{kq}$  are the spherical

harmonics. The  $\rho_{kq}(t)$  are the statistical tensor elements describing the initial orientation (polarization) of the nuclear state ( $t = 0$ ) and its change in time by the EQI and magnetic HFI as expressed by

$$\rho_{kq}(t) = \sum_{k'q'} G_{kk'}^{qq'}(t) \cdot \rho_{k'q'}(t = 0). \quad (5)$$

The coefficients  $G_{kk'}^{qq'}(t)$  reduce in our case where the  $z$  axis coincides with the direction of the TEFG, to  $G_{kk'}^{qq}(t)$  and must be replaced by their time integrated values:

$$G_{kk'}^{qq}(T) = \frac{\int_0^T G_{kk'}^{qq}(t) e^{-t/\tau} dt}{\int_0^T e^{-t/\tau} dt} = G_{kk'}^{\text{TEFG}}(\omega_Q T), \quad (6)$$

where

$$\omega_Q = \frac{eQV_{ZZ}}{4\hbar I(2I - 1)} \quad (7)$$

is the quadrupole frequency depending on the nuclear spin  $I = 2$ , the quadrupole moment  $Q(2^+)$ , and the electric field gradient  $V_{ZZ}^{\text{TEFG}}$ . The perturbation coefficients of the magnetic HFI in vacuum enter in Eq. (4) as a factor (due to the sequential nature of the EQI and magnetic HFI) being characterized by  $G_{kk'}^{\text{vac}}(t = \infty)$  with time integration from the time of emergence into vacuum to infinity. Applying this procedure to both angular correlations the least squares fit to the data yielded for the TEFG with definitely positive sign a mean value

$$V_{ZZ}(^{32}\text{S}) = +5.3(1.3) \times 10^{21} \text{ V/cm}^2$$

and for the quadrupole precession angle [Eq. (7)]

$$\omega_Q T = -16(4) \text{ mrad},$$

where the negative sign results from the quadrupole moment.

Finally, we obtained for the attenuation coefficients due to the magnetic HFI in vacuum the values

$$G_2^{\text{vac}} = 0.97(2) \quad \text{and} \quad G_4^{\text{vac}} = 0.88(5),$$

which are well explained by the strong hyperfine fields of electron configurations of H-like and He-like ions formed on emergence into vacuum (see [5,12]).

TABLE I. Relevant parameters for the determination of the electric quadrupole interactions in transient electric field gradients (see text).

Nucleus	Host <sup>a</sup>	$Q(2^+)$ (eb) <sup>b</sup>	$T$ (ps)	$\omega_Q T$ (mrad)	$V_{ZZ}^{\text{TEFG}}$ ( $10^{21} \text{ V/cm}^2$ ) <sup>c</sup>	$V_{ZZ}^{\text{calc}}$ ( $10^{21} \text{ V/cm}^2$ ) <sup>d</sup>
$^{20}\text{Ne}(2^+)$	Ag/Gd	-0.23(3)	0.51(5)	-2(3)	0.3(4)	0.6
$^{32}\text{S}(2^+)$	Gd	-0.149(13)	0.31(3)	-16(4)	5.3(1.3)	2.5
$^{40}\text{Ar}(2^+)$	Pb/Gd	+0.02	0.30(3)	+8(5)	20(12)	3.5
$^{52}\text{Cr}(2^+)$	Gd	-0.082(16)	0.32(3)	-3(2)	1.9(1.4)	8.3
$^{54}\text{Fe}(2^+)$	Pb/Gd	-0.05(8)	0.25(2)	-3(4)	4(5)	10.5
$^{62}\text{Ni}(2^+)$	Pb/Fe	-0.05	0.26(2)	-6(4)	8(4)	13.2

<sup>a</sup>Main components.

<sup>b</sup>Exp. data [19], values without error refer to shell model calculations [17,18].

<sup>c</sup>Errors quoted are of statistical origin.

<sup>d</sup>Calculated with Eq. (3).

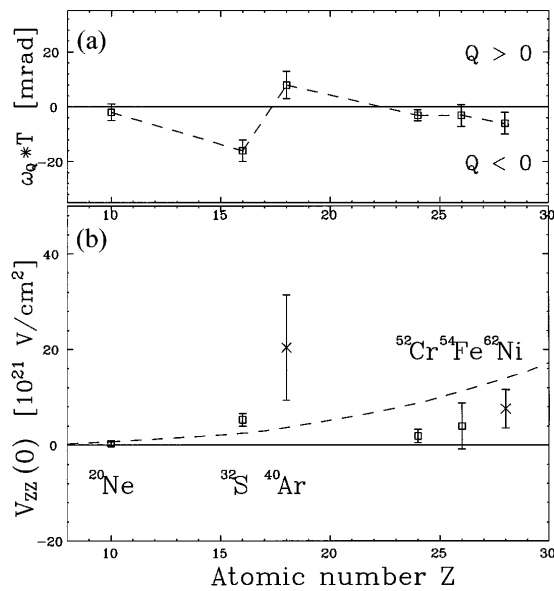


FIG. 4. (a) Deduced  $(\omega_Q T)$  values distinguishing between different signs of the quadrupole moment; lines are to guide the eye. (b) Measured TEFG as a function of the atomic number of the ion. The dashed line represents predictions by Eq. (3);  $x$  symbols refer to calculated  $Q$ . The error bars do not include uncertainties in  $Q$ .

The same analysis was applied to the angular correlation data of the other nuclei in the study yielding similar results (Table I and Fig. 4). It is noted that the sign of the quadrupole moments is well determined supporting theoretical estimates [17,18] where the experimental data are not conclusive. In fact, the present analysis allowed us to determine unambiguously the sign of the quadrupole moment for  $^{40}\text{Ar}(2^+)$  ( $Q > 0$ ) and  $^{62}\text{Ni}(2^+)$  ( $Q < 0$ ).

In summary, for the first time we have data showing the definite existence of TEFG which had been searched for a long time. The most significant information comes from H-like  $^{32}\text{S}(2^+)$  ions which gave clear evidence for this phenomenon. The strength of the field gradients of highly ionized ions of  $10^{21}$  V/cm<sup>2</sup> is sufficiently intense to measure quadrupole moments of nuclear levels with ps lifetimes. The positive sign of the TEFG opposite to that of the wake field gradient is in accordance with the Sternheimer effect.

The authors are indebted to L. Zamick (Rutgers University) for providing calculations of quadrupole moments. They are grateful to M. Forker (ISKP, University of Bonn) and R.L. Rasera (UMBC, University of Maryland) for many illuminating discussions. Support by

the BMBF and the Deutsche Forschungsgemeinschaft is acknowledged.

- [1] J. Lindhard and A. Winther, Nucl. Phys. **A166**, 413 (1971).
- [2] Z. Vager and D.S. Gemmell, Phys. Rev. Lett. **37**, 1352 (1976).
- [3] H. Ernst, W. Henning, T.J. Humanic, T.L. Khoo, S.C. Pieper, and J.P. Schiffer, Phys. Rev. C **26**, 2039 (1982).
- [4] W. Korten, J. Gerl, D. Habs, and D. Schwalm, Z. Phys. A **339**, 217 (1991).
- [5] J. Cub, M. Bussas, K.-H. Speidel, W. Karle, U. Knopp, H. Busch, H.-J. Wollersheim, J. Gerl, K. Vetter, C. Ender, F. Köck, J. Gerber, and F. Hagelberg, Z. Phys. A **345**, 1 (1993).
- [6] F.D. Feiock and W.R. Johnson, Phys. Rev. **187**, 39 (1969).
- [7] L. Grodzins and O. Klepper, Phys. Rev. C **3**, 1019 (1971).
- [8] N. Benczer-Koller, M. Hass, and J. Sak, Annu. Rev. Nucl. Part. Sci. **30**, 53 (1980).
- [9] J. Cub, U. Knopp, K.-H. Speidel, H. Busch, S. Kremeyer, H.-J. Wollersheim, N. Martin, X. Hong, K. Vetter, N. Gollwitzer, A.I. Levon, and A. Booten, Nucl. Phys. **A549**, 304 (1992).
- [10] K.-H. Speidel, J. Cub, U. Reuter, F. Passek, H.-J. Wollersheim, N. Martin, P. Egelhof, H. Emling, W. Henning, R.S. Simon, H.-J. Simonis, and N. Gollwitzer, Z. Phys. A **339**, 265 (1991).
- [11] U. Grabowy, K.-H. Speidel, J. Cub, H. Busch, H.-J. Wollersheim, G. Jakob, A. Gohla, J. Gerber, and M. Loewe, Z. Phys. A (to be published).
- [12] J. Cub, Ph.D. thesis, Report No. GSI-93-27, 1993.
- [13] K.-H. Speidel, J. Cub, M. Knopp, H.-J. Simonis, H.-J. Wollersheim, P. Egelhof, H. Emling, H. Grein, W. Henning, R. Holzmann, R.S. Simon, R. Schmidt, and N. Gollwitzer, Hyperfine Interact. **61**, 1343 (1990).
- [14] J.F. Ziegler, J. Biersack, and U. Littmark, *The Stopping and Range of Ions in Solids* (Pergamon, Oxford, 1985), Vol. 1.
- [15] A. Winther and J. de Boer, in *Coulomb Excitation*, edited by K. Alder and A. Winther (Academic Press, New York, 1966), p. 303.
- [16] H. Frauenfelder and R.M. Steffen, in *Alpha-, Beta- and Gamma-Ray Spectroscopy*, edited by K. Siegbahn (North-Holland, Amsterdam, 1965), Vol. 2.
- [17] L. Zamick (private communication).
- [18] P.W.M. Glaudemans, M.J.A. de Voigt, and E.F.M. Steffens, Nucl. Phys. **A198**, 609 (1972).
- [19] P. Raghavan, At. Data Nucl. Data Tables **42**, 189 (1989).